

Impact of Intermetallic Growth on the Mechanical Strength of Pb-Free BGA Assemblies

Patrick Roubaud, Grace Ng, Greg Henshall – Hewlett Packard
Ronald Bulwith, Robert Herber - Alpha Metals
Swaminath Prasad, Flynn Carson – ChipPAC
Sundar Kamath, Alexander Garcia – Sanmina

Presented at APEX 2001 on January 16-18, 2001 in San Diego, CA

ABSTRACT

The increasing industry awareness of lead-free activities has prompted users and suppliers to investigate lead-free solder systems in detail. The need to understand the intermetallic formation, structure, and its impact on the reliability of solder joints was the driving force behind this study. If intermetallics grow to sufficient thickness, fracture can occur during handling, shipping or service. This problem has been studied in detail for the tin-lead solder system, but it is not well understood for candidate lead-free solders.

Test boards populated with SMT lead-free components have been aged at 125° C and 150° C for intervals of time up to 32 days. The printed circuit boards had OSP surface finish. Four ball metallurgies (Sn-Ag, Sn-Cu, Sn-Ag-Cu and Sn-Ag-Cu-Bi) have been evaluated for the Plastic Ball Grid Array (PBGA) packages. The solder paste used in the SMT process was the Sn-Ag-Cu. The thickness of the intermetallics has been measured for each time interval and the activation energy for their growth has been computed. Additionally, these interconnections have been screened for catastrophic failure using 4-point bend tests, and compared with parts soldered with conventional Sn-Pb solder. The implications of these results for the reliability of lead-free interconnections are discussed.

Introduction

Eutectic Tin-Lead solder became a de-facto standard in the electronic industry because of its unique combination of material properties and low cost. In recent years, environmental concerns have been raised regarding the use of lead-containing solder in electronic products. The European community has a proposed Waste in Electronic and Electric Equipment (WEEE) Directive that restricts the intentional use of lead in electronic products after January 1, 2008. The European Parliament has not yet approved the WEEE Directive. Nonetheless, movement away from lead-bearing solder is advancing, driven

mainly by competitive pressures in consumer electronics and concerns about the lead in discarded electronic products. In Japan, the Japan Electronic Industry Development Association (JEIDA) published a road map to achieve lead replacement by 2005 [1]. In this effort toward lead elimination, a variety of Pb-free printed circuit board (PCB) finishes, package lead surface finishes, and Pb-free Ball Grid Array (BGA) metallurgies have been developed. It is not clear how the properties of the solder joints will be altered when the Pb-free solders interact with these newly developed metallurgical surfaces. For example, the effect of alloying elements on the aging behavior is not well understood. Furthermore, the temperatures used during most lead-free soldering processes are higher than those used in corresponding Sn-Pb process, which may lead to thick intermetallic layers. Those intermetallics are brittle and may compromise the joint's mechanical integrity, leading to failure at unacceptably low mechanical stresses, such as those potentially applied during shipping, handling, or mild mechanical shock. Since the trend in modern electronics is miniaturizing solder joints, the role of these compounds may become more important as the thickness of the bulk solder is reduced. Therefore, it is important to determine if lead-free solder joints are subject to intermetallic growth kinetics significantly faster than that of Sn-Pb and whether these compounds lead to fragile joints.

Intermetallic Growth Kinetics

Experimental Procedure

388 I/O PBGAs packages, specially developed for the lead-free process [2], were used for this study. These packages were ball attached with either the standard 63Sn-37Pb alloy or one of four lead-free alloys selected for this study. The PBGAs were then attached to conventional PCBs using the standard 63Sn-37Pb (peak temperature during assembly: 220° C) and a lead-free Sn-4Ag-0.5Cu (peak temperature during assembly: 250° C) solder paste. The boards had a lead-free Organic Solder Preservative (OSP) finish and the pads were non-soldermask defined (NSMD). More details about the package, the boards and the assembling process can be found in [3].

The thermal aging of the samples was performed in air at temperatures of 125° C (+/- 1.1° C) and 150° C (+/- 1.1° C). For this aging study, 84 samples divided into the 6 different combinations listed in Table 1 were built. After 1, 2, 4, 8, 16 and 32 days, samples of each type were removed for metallographic examination. A sample of each type was also examined without aging (aging time = 0 day) to serve as a baseline.

BGA Solder Ball Metallurgies	Surface Mount Solder Paste	Peak temperature during the Assembly Process (°C)
63Sn-37Pb	63Sn-37Pb	220
63Sn-37Pb	Sn-4.0Ag-0.5Cu	250
Sn-4.0Ag-0.5Cu		
Sn-2.5Ag-1.0Bi-0.5 Cu		
Sn-0.75 Cu		
Sn-3.5Ag		

Table 1 – Samples for the activation energy and the 4-point bending tests.

The BGAs were removed from the motherboard using a handheld 'Dremel' cutting tool. A low speed diamond saw was used to cut through the component and expose the solder connections for metallographic preparation. The component segments were then potted in a low exotherm metallographic potting compound as to minimize the introduction of thermal artifacts on the solder microstructure. Once the sample was potted and marked with the appropriate identification, it was roughly ground to the proximity of the solder connections to be examined with an 80 grit abrasive belt. Further wet grinding on successively finer grit abrasive papers was carried out from 240 grit through 600 grit abrasives. Following the grinding, the samples were successively polished with 3 micron and then 1/4 micron diamond abrasives on a rotating polishing wheel covered with a synthetic polishing cloth. The final polishing step was then carried out on an automated vibratory polishing table using a 0.05-micron Alumina abrasive. The samples were then etched to more clearly reveal the reaction interfaces with the solder for the microscopic examination and the measurements of intermetallic layers thickness. Microscopic examination was carried out using a Zeiss Ultraphot II metallurgical microscope fitted with Optronics digital cameras and image capture software.

Results and Discussion

Figure 1 shows a general view of a lead-free solder joint. The Cu_6Sn_5 intermetallic sublayer is clearly visible on each sample. The Cu_3Sn sublayer is noticeable only for the sample annealed at 150°C . Figure 2 contains a micrograph of a lead-free ball aged at 150°C for 32 days.

Comparison of the 63Sn-37Pb joints and the lead-free joints shows that the initial thickness of the intermetallic layer is not significantly impacted by the higher temperature used during the lead-free assembly process. All the values are in a range of 1.6 to 2.3 microns, as shown in Figure 3.

The growth of these intermetallic layers can be modeled using parabolic growth kinetics [4]:

$$w = w_0 + D\sqrt{t} \quad (1)$$

Where: w = thickness of the intermetallic layer
 w_0 = initial thickness of the layer
 D = Diffusion coefficient
 t = time

Figure 4 shows the intermetallic layer growth as a function of the square root of the annealing time. The straight lines represent a linear regression plot of the total intermetallic thickness (i.e. the combined thickness of the Cu_6Sn_5 and Cu_3Sn sublayers). These data indicate that the intermetallic layer growth is comparable from one sample to another. There are no significant differences in growth rate due to the paste metallurgy, the ball metallurgy or the peak temperature during the reflow process. Although these

data are limited, it does not appear that intermetallic layer growth is faster for the lead-free joints than for the control Sn-Pb joints, and may in fact be somewhat slower.

For each joint type, D was measured from the slopes in figure 4 at 32 days. The activation energy Q was measured assuming Arrhenius behavior, by plotting $\ln(D)$ versus $1/T$. The results are reported in Table 2.

Surface Mount Solder Paste	BGA Solder Ball Metallurgies	Activation Energy (kJ/mol)
63Sn-37Pb	63Sn-37Pb	45
Sn-4.0Ag-0.5Cu	63Sn-37Pb	48
	Sn-4.0Ag-0.5Cu	33
	Sn-2.5Ag-1.0Bi-0.5 Cu	68
	Sn-0.75 Cu	50
	Sn-3.5Ag	31

Table 2 – Measured Activation energies for the solder joint type investigated.

The value obtained for the Sn-Pb system (45 kJ/mol) was found to be in accordance with the literature [5]. Qualitatively, it appears that the activation energies for the lead-free solders are within approximately +/- 50% of the value for 63Sn-37Pb. It also appears that the joints containing the highest amount of Ag (Sn-3.5Ag and Sn-4.0Ag-0.5Cu) have the lowest activation energy. However, the scope of this study does not allow us to draw definite quantitative conclusions. The small number of test points and the design of the samples prevent us from doing so. In addition, we did not separate the contributions from the Cu_3Sn and Cu_6Sn_5 sublayers.

Mechanical Strength

As a preliminary investigation of the mechanical strength of Pb-free interconnects, four-point bending tests were performed to simulate the shipping and handling environment. Note that these tests were not meant to investigate the thermal fatigue or creep properties of the solder joints. Such investigations are underway and will be reported elsewhere.

Experimental Procedure

The test vehicle consisted of a 35mm x 35mm, daisy-chained 388 I/O PBGA package mounted on a 203 x 72 mm PCB. The four lead-free metallurgies described previously were used for the balls of the BGAs, and the Sn-4Ag-0.5Cu lead-free solder paste was used to attach the parts on the PCB. For control, BGAs with traditional 63Sn-37Pb solder balls were also assembled, with 63Sn-37Pb solder paste and with the Sn-4Ag-0.5Cu lead-free solder paste. In all cases OSP was used as the board finish.

The assemblies were tested in 4-point bending on a screw-driven Instron testing machine (model # 5566). The crosshead speed was set to 0.762 mm/min (0.03 in/min). Figure 5

illustrates the experimental setup. A total of 4 samples per joint metallurgy (see Table 1) were tested. A multi-meter was used to monitor the continuity of electrical signals during the experiment. The BGA assemblies were tested to failure – either discontinuity of electrical signal or separation of the BGA from the PCB. The experiments were run at room temperature.

Results and Discussion

A representative load vs. displacement plot for the 4-point bend test is shown in Figure 6. As a test assembly was loaded, the load vs. displacement plot followed a relatively straight line as both the PCB and BGA were bent. The load ultimately reached a maximum value, where the BGA separated from the board, and then decreased. The maximum load is defined as the fracture load.

Table 3 lists the average fracture load for the Pb-free solder joints and the Sn-Pb control. Based on the results, the alloys can be broken into two groups. Joints containing Sn-2.5Ag-1.0Bi-0.5Cu and Sn-3.5Ag alloys exhibited fracture loads in the range of 600N to 700N, similar to those with the eutectic 63Sn-37Pb. The second group, consisting of Sn-Ag-Cu and Sn-Cu, exhibited fracture loads ranging from 900N to 1050N. Standard deviations for the average fracture load of each alloy ranged from 27N-190N.

Paste	BGA	Sample #	Average Fracture Load (N)	Standard Deviation
Sn-Pb	63Sn-37Pb	1 2 3 4	691.6	93.3
Sn-Ag-Cu	63Sn-37Pb	5 6 7 8	655.6	102.5
	Sn-4.0Ag-0.5Cu	9 10 11 12	935.0	190.4
	Sn-2.5Ag-1.0Bi-0.5 Cu	13 14 15 16	682.5	27.3
	Sn-0.75 Cu	17 18 19 20	1046.9	125.6
	Sn-3.5Ag	21 22 23 24	716.4	126.3

Table 3 – Average and standard deviation of fracture load for Sn-Pb control and Pb-free Alloys

All of the samples exhibited the same failure mode. The copper pads, along with some adjacent epoxy, were pulled out of the PCBs. Figure 7 provides a schematic drawing of this pad-pull-out failure mode. Figure 8(a) shows the fracture surface on the PCB side where the copper pads were pulled out, revealing the fiberglass underneath. Figure 8(b) is the mirror image on the BGA side. The copper traces and pads were pulled out of the PCB during the mechanical flexure test. Epoxy residue on the copper traces/pads showed imprints of the fiberglass that was underneath.

In some rare cases, the corner solder joint exhibited an interfacial fracture or a pad-pull-out fracture on the BGA package side. Interfacial fracture of a corner joint was observed for the Sn-0.75Cu and Sn-3.5Ag alloys. Figures 9 illustrates this failure mode.

The pad-pull-out failure mode observed for the vast majority of samples indicates that the Pb-free solder joints are mechanically sound. Aside from the few cases of interfacial fractures along the corner solder joints, the solder joints were stronger than the epoxy holding the Cu pads to the PCB. Even in cases of interfacial fracture, the measured

fracture load was as high as that exhibited by the eutectic Sn-Pb control. Therefore, the interface between the solder and the BGA or PCB can withstand a substantial amount of stress.

Since all but a few samples exhibited the pad-pull-out failure mode, one would expect similar fracture loads across the samples. However, the results showed two distinct groups of fracture load. Due to the small number of test samples and the large standard deviation within each group of alloy, a conclusive quantitative comparison of the mechanical strength of Pb-free solders and eutectic Sn-Pb solder cannot be drawn.

Conclusions

For the combinations of solder joint metallurgies studied, the following conclusions can be drawn:

1. The high temperature (250° C) reached during the lead-free assembly process does not lead to a significantly higher thickness of the intermetallic layer at the junction between the solder and the copper substrate.
2. After 32 days of annealing, the thicknesses of the intermetallic layers for the lead-free joints are slightly smaller than those for 63Sn-37Pb.
3. Four-point bend testing experiments showed that the lead-free joints are mechanically as sound as the joints made with 63Sn-37Pb.

These combined results indicate that the higher assembly process temperature, the nature of the lead-free ball metallurgies and the lead-free solder paste are not a concern regarding the quantity and the brittleness of the intermetallics for the joint systems studied. Therefore, the reliability of these lead-free systems can be pursued with more extensive tests, such as accelerated thermal cycling.

Acknowledgments

The authors would like to acknowledge Jerry Ortkiese of HP and Fay Hua formerly with HP, now with Intel Corporation, for their continuous support and suggestions.

REFERENCES

[1] <http://www.jeida.or.jp/english/information/pbfree/roadmap.html>

[2] S. Prasad, F. Carson, J.S. Lee, T.S. Jeong, Y.S. Kim, "Reliability of Lead Free BGA Packages", Proceedings of IMAPS, Boston September 2000

[3] S. Prasad, F. Carson, G.S. Kim, J.S. Lee, P. Roubaud, G. Henshall, S. Kunder, A. Garcia, R. Herber, R. Bulwith., "Board Level Reliability of Lead-Free Packages", Proceedings of SMTA, Chicago September 2000, pp 272-276

[4] Wassink, R. J. Klein, Soldering in Electronics, 2nd ed., 1989, Electrochemical Publications Limited, Ayr, Scotland.

[5] P.T. Vianco, K.L. Erickson, P.L. Hopkins, "Solid State Intermetallic Compound Growth Between Copper and High Temperature, Tin-Rich Solders", Journal of Electronic Materials, Vol.23, No 8, 1994, p. 721

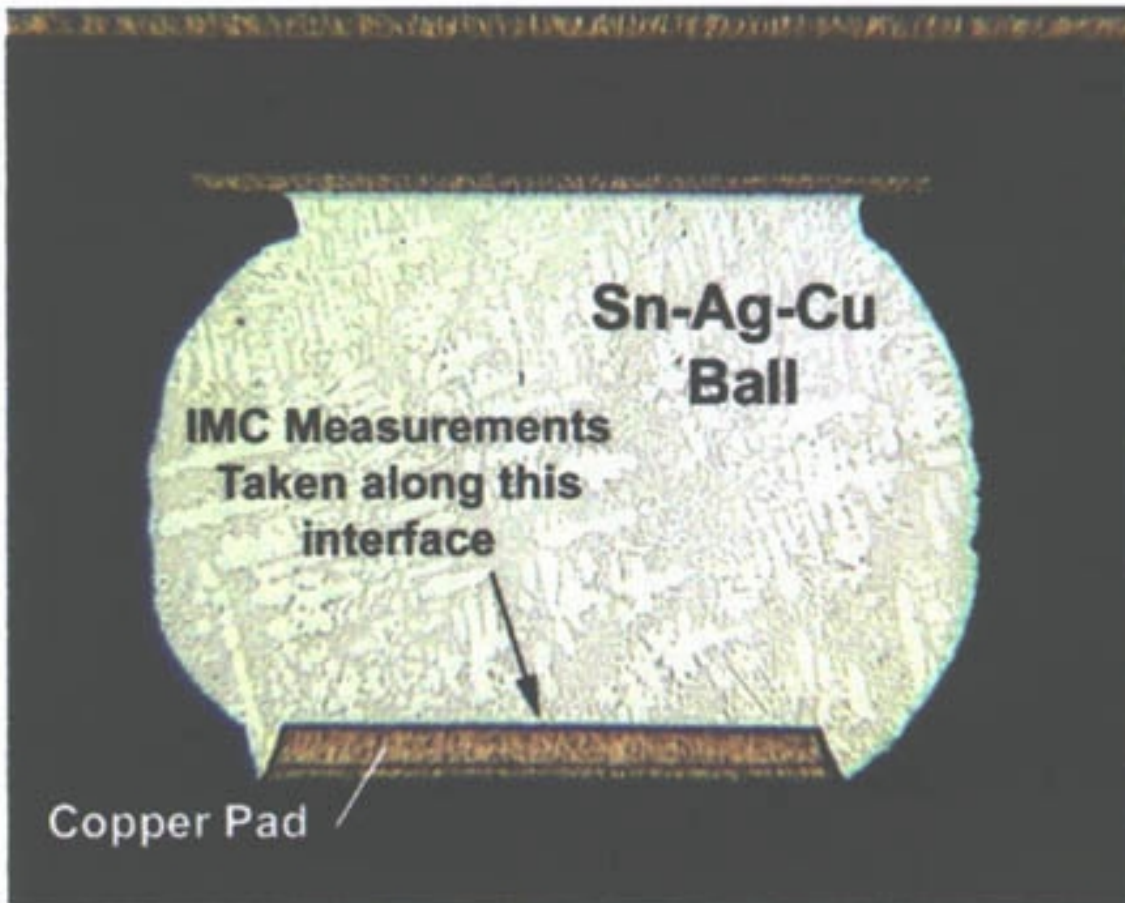


Fig.1 - Micrograph of a lead free solder joint (Sn-4.0Ag-0.5Cu used for the ball metallurgy and the solder paste).

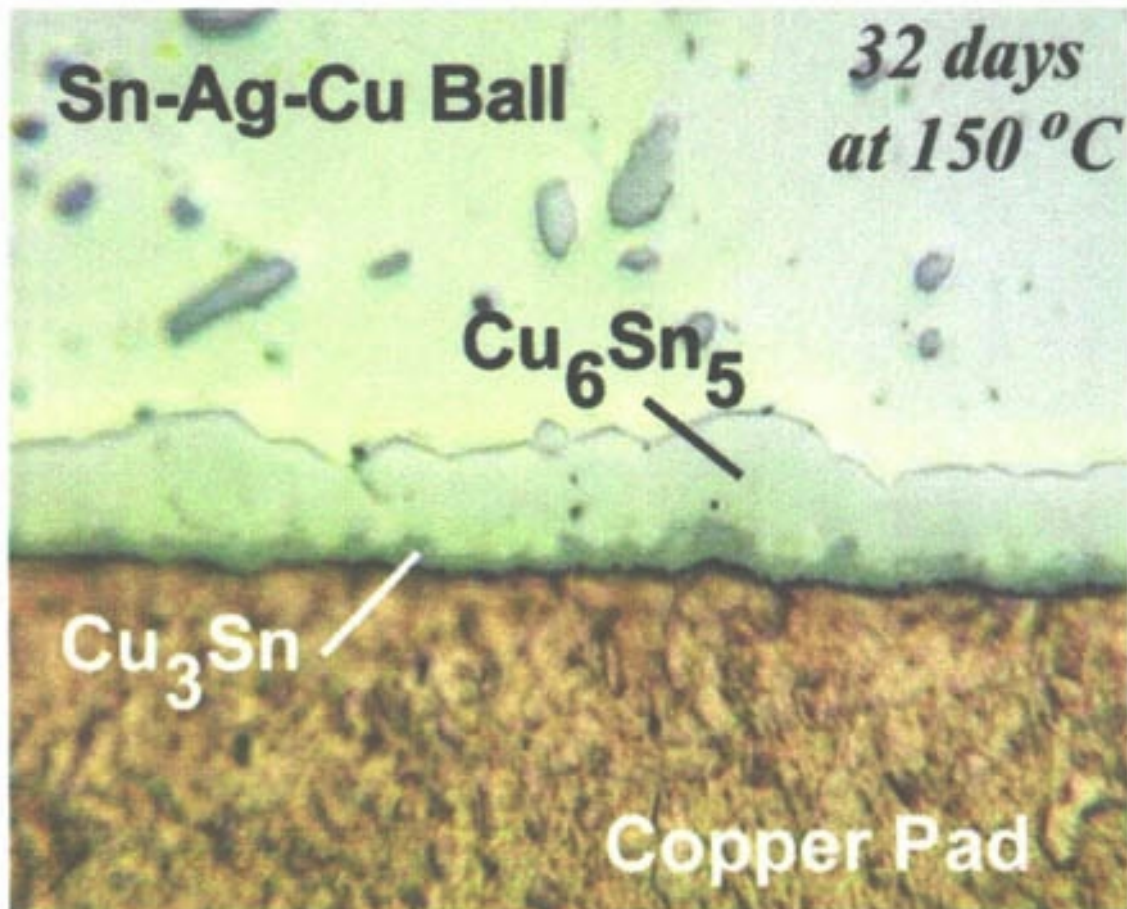


Fig. 2 – Intermetallic compounds at the interface of the copper pad and a Sn-4Ag-0.5Cu ball after 32 days of aging at 150°C.

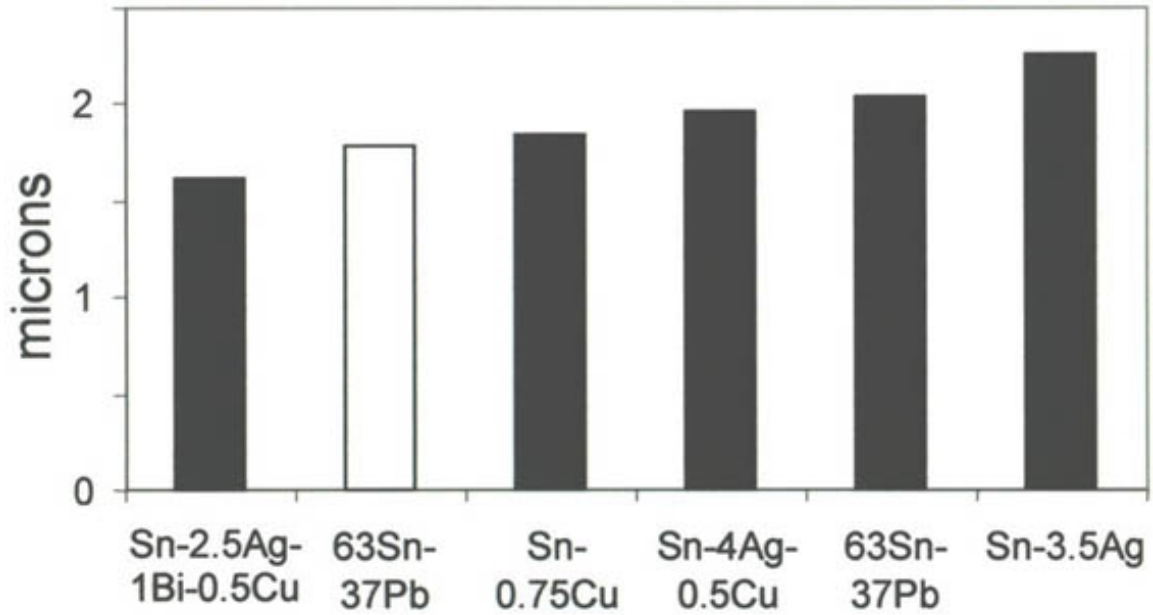


Fig. 3— Initial thickness of the initial intermetallic layers. The white bar represents the PBGA attached with 63Sn37-37Pb solder paste (peak reflow temperature: 220°C). The other PBGA were attached with Sn-4Ag-0.5Cu (peak reflow temperature: 250°C)

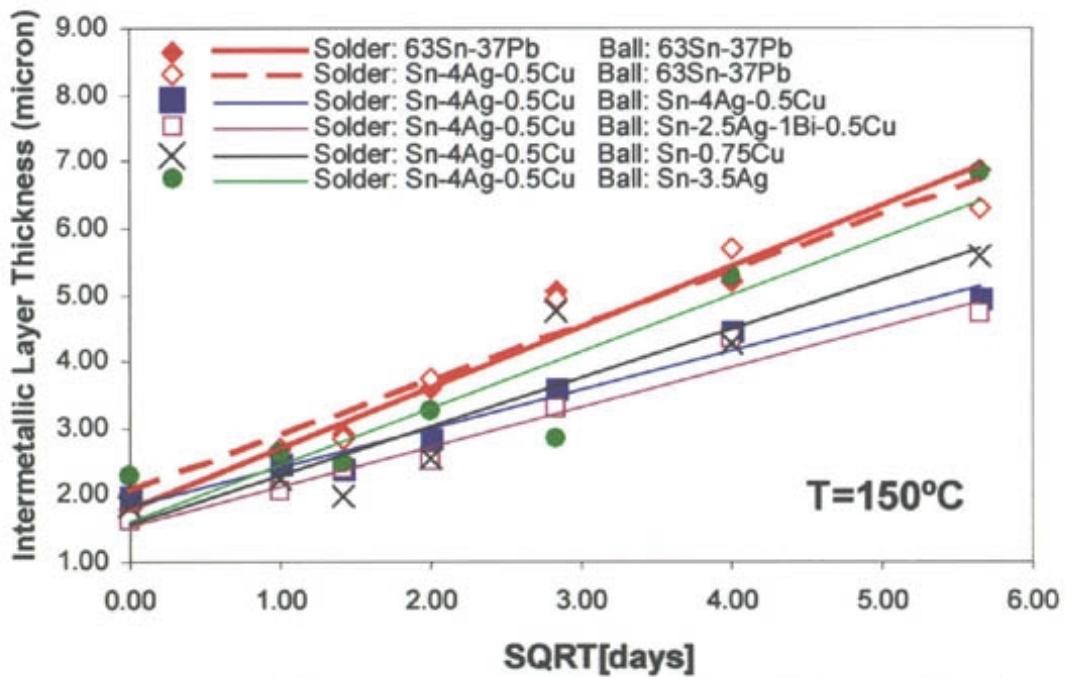
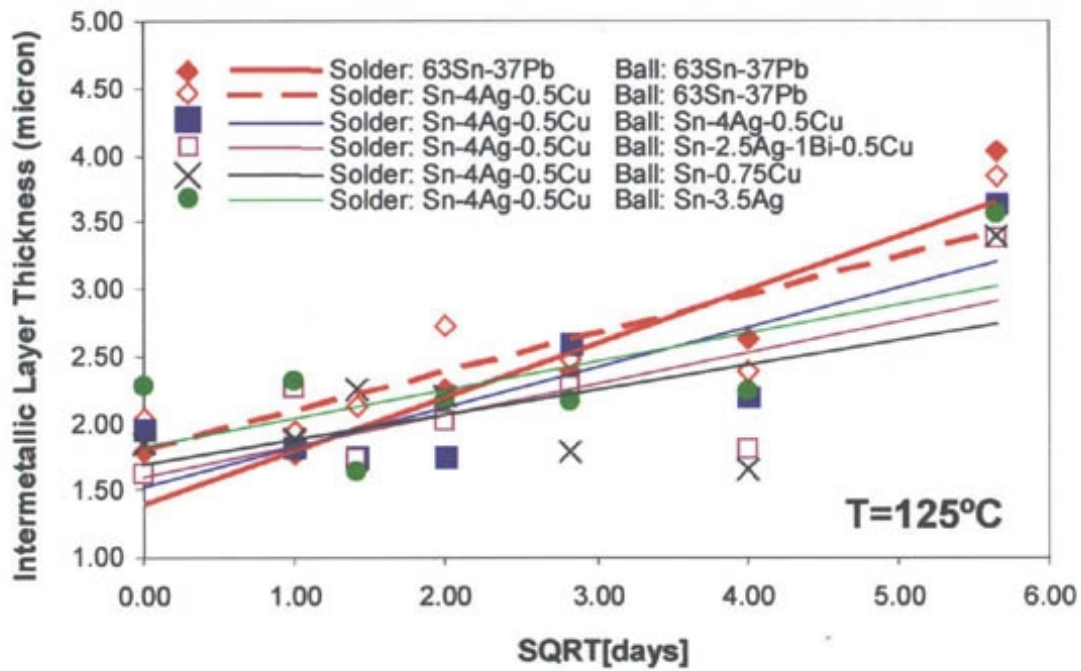


Fig.4 - Intermetallic thicknesses versus the square root of the annealing time (in days). The straight line represent a linear regression plot of the total intermetallic thickness.

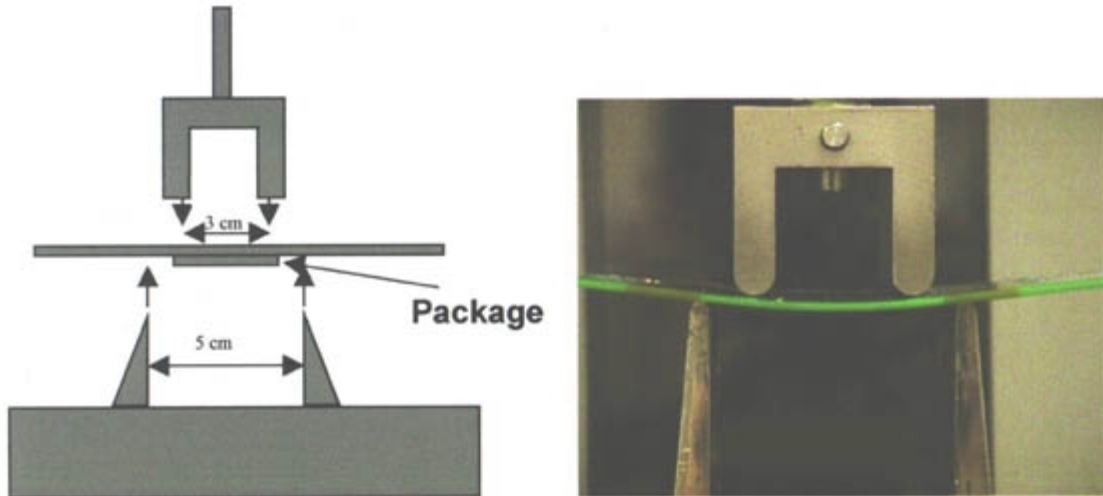


Fig. 5 - A schematic drawing and a photograph of the 4-point bend test setup

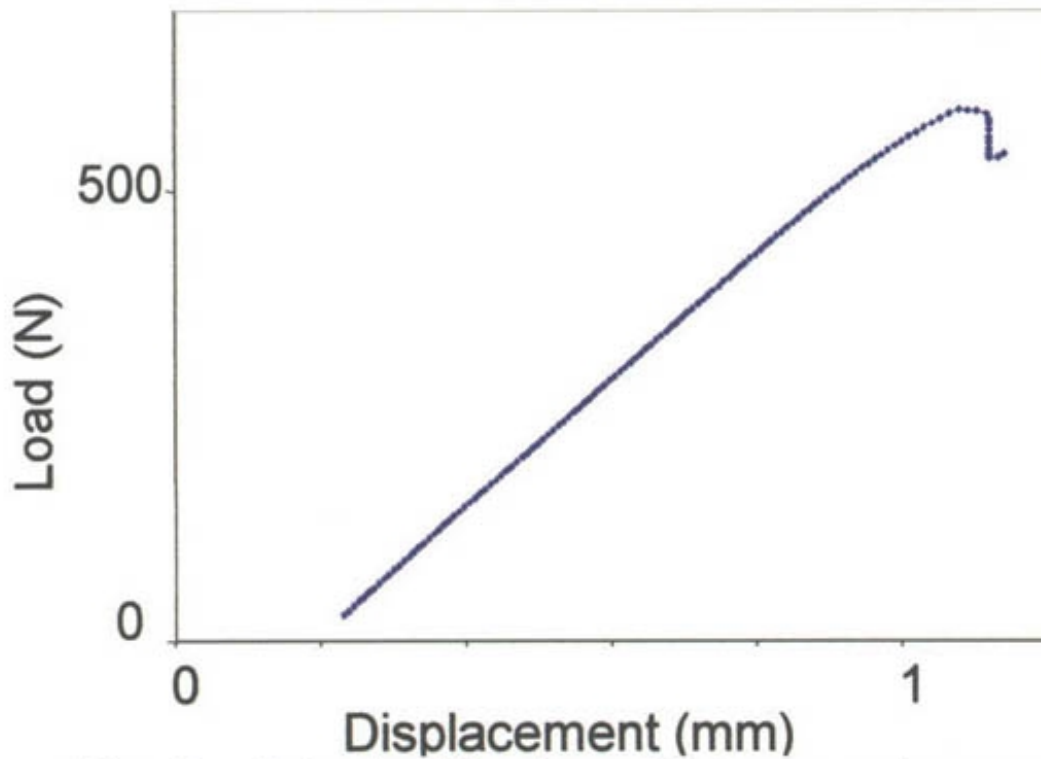


Fig. 6 – A typical load vs. displacement curve. Notice the change in slope at the peak (failure load).

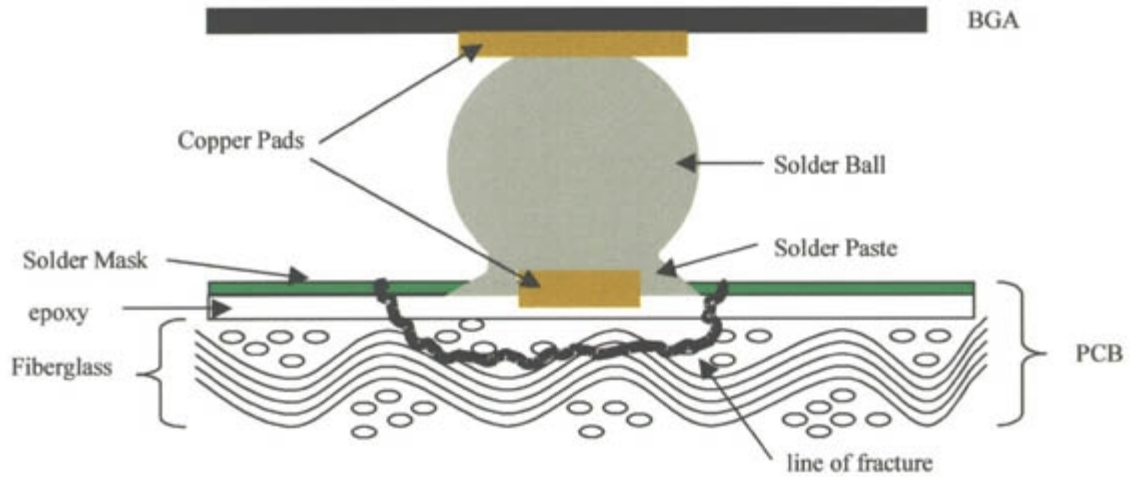


Fig. 7 – A schematic drawing of a pad-pull-out fracture. The copper pad along with the epoxy was pulled out of the PCB along the line of fracture.

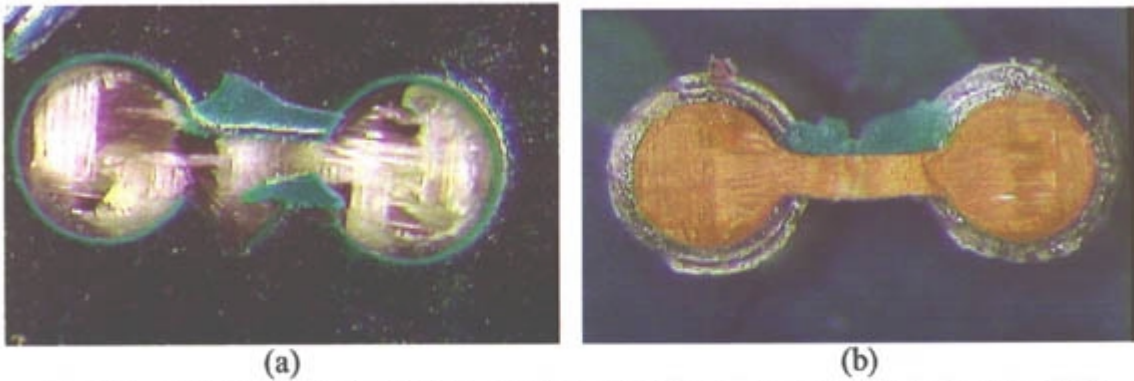


Fig. 8 – A close-up of the fracture surface. (a) Fiberglass was revealed on the PCB after the copper pads were pulled out. (b) Both copper traces and copper pads were pulled out. Epoxy residue on the copper showed imprints of fiberglass.

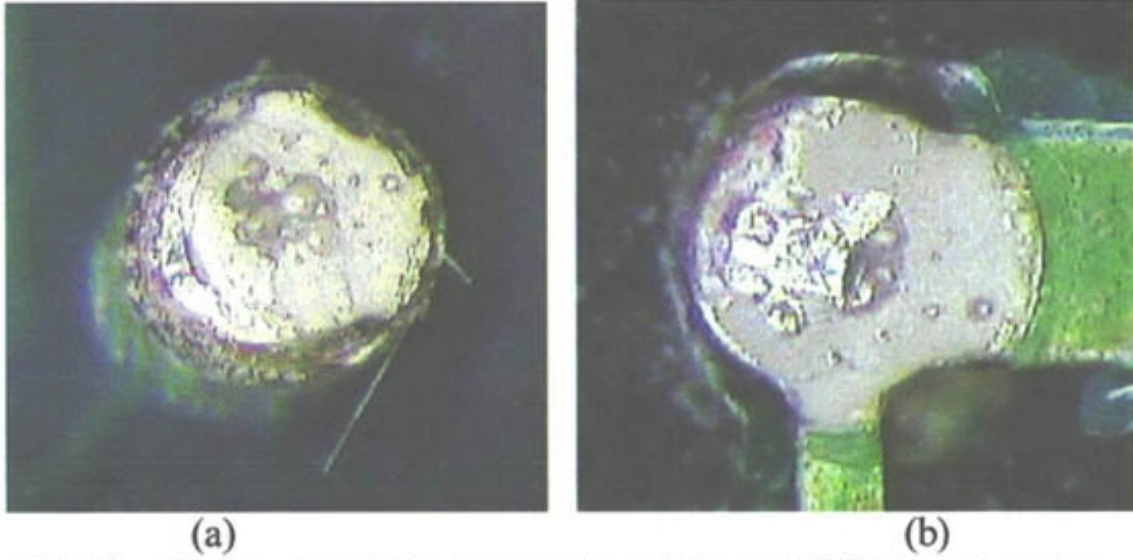


Fig. 9 – An interfacial fracture on the solder and PCB interface for a Sn-Ag solder joint. **(a)** Solder interface on the BGA. **(b)** Solder interface on the PCB